

The Detectability of Ly α Emission from Galaxies during the Epoch of Reionization

Mark Dijkstra^{1*}, Andrei Mesinger^{2†} and J. Stuart B. Wyithe³

¹Max Planck Institute for Astrophysik, Karl-Schwarzschild-Str. 1, 85741 Garching, Germany

²Department of Astrophysical Sciences, Princeton University, Princeton, NJ 08544, USA

³School of Physics, University of Melbourne, Parkville, Victoria, 3010, Australia

30 October 2018

ABSTRACT

We study the visibility of the Ly α emission line during the Epoch of Reionization (EoR). Combining galactic outflow models with large-scale semi-numeric simulations of reionization, we quantify the probability distribution function (PDF) of the fraction of Ly α photons transmitted through the intergalactic medium (IGM), \mathcal{T}_{IGM} . Our study focusses on galaxies populating dark matter halos with masses of $M_{\text{halo}} = 10^{10} M_{\odot}$ at $z = 8.6$, which is inspired by the recent reported discovery of a galaxy at $z = 8.6$ with strong Ly α line emission. For reasonable assumptions, we find that the combination of winds and reionization morphology results in $\mathcal{T}_{\text{IGM}} \gtrsim 10\%$ [50%], for the majority of galaxies, even when the Universe is $\sim 80\%$ [60%] neutral by volume. Thus, the observed strong Ly α emission from the reported $z = 8.6$ galaxy is consistent with a highly neutral IGM, and cannot be used to place statistically significant constraints on the volume averaged neutral fraction of hydrogen in the IGM. We also investigate the implications of the recent tentative evidence for a observed decrease in the ‘Lyman Alpha Emitter fraction’ among drop-out galaxies between $z = 6$ and $z = 7$. If confirmed, we show that a rapid evolution in \bar{x}_{HI} will be required to explain this observation via the effects of reionization.

Key words: galaxies: high redshift – galaxies: stellar content; cosmology: dark ages, reionization, first stars – cosmology; early Universe – cosmology; diffuse radiation – cosmology; large-scale structure of Universe – radiative transfer

1 INTRODUCTION

The Wide Field Camera 3 on board of the *Hubble Space Telescope* has enhanced our ability to observe galaxies at redshifts great than six, so-far obtaining ~ 100 likely candidate galaxies at $z = 7, 8$ (e.g. Bouwens et al. 2010a; Bunker et al. 2010; Finkelstein et al. 2010; Yan et al. 2010). The *James Webb Space Telescope* is expected to probe galaxies a few magnitudes deeper, and also to spectroscopically confirm the redshifts of the existing candidates. One of the key predicted properties of young, metal poor galaxies in the high-redshift Universe are prominent nebular emission lines, dominated by hydrogen Ly α ($\lambda = 1216 \text{ \AA}$, see e.g. Johnson et al. 2009, Pawlik et al. 2010). The first generation of galaxies are likely to have been strong Ly α emitters, with equivalent widths possibly as high as $\text{EW} \sim 1500 \text{ \AA}$ (Schaerer 2002, 2003; Johnson et al. 2009, also see Partridge & Peebles 1967).

During the epoch of reionization (EoR), the Ly α emission line may be difficult to observe, due to the large opacity of the intervening neutral intergalactic medium: for example, a source needs to be embedded in a $\gtrsim 1$ Mpc HII region to allow Ly α photons to redshift far away from the line center before they reach the IGM (e.g., Miralda-Escude 1998; Cen & Haiman 2000). For the galaxy to generate such a large HII region, its ionizing luminosity would have to be unphysically large (unless there is a bright quasar associated with the galaxy, see Cen & Haiman 2000). However, several effects have been shown to boost the detectability of the Ly α flux: (*i*) source clustering, which boosts the sizes of HII regions (Furlanetto et al. 2004; Mesinger & Furlanetto 2008b; McQuinn et al. 2007; Iliev et al. 2008) (*ii*) the patchiness of reionization, which may give rise to significant fluctuations in the IGM opacity between different sightlines, as well as a steeper absorption profile (e.g., Mesinger & Furlanetto 2008a; McQuinn et al. 2008), and (*iii*) radiative transfer effects through outflows of interstellar (ISM) H I gas, which

* E-mail: dijkstra@mpa-garching.mpg.de

† Hubble Fellow; E-mail: mesinger@astro.princeton.edu

can impart a redshift¹ to the Ly α photons before they emerge from galaxies (Santos 2004; Dijkstra & Wyithe 2010, but also see Barnes et al. 2011).

Lehnert et al. (2010) recently reported a detection of strong Ly α line emission from a Y_{105} drop-out galaxy in Wide Field Camera 3 observations of the Hubble Ultra Deep Field. The Ly α line implies that the galaxy is at $z \sim 8.56$, which is the highest redshift of any spectroscopically-confirmed object to date. Interestingly, when taken at face value, the observed Ly α line is strong, with an observed equivalent width (EW) of $\sim 100 \text{ \AA}$ (see § 4). Motivated by this observation, we study the visibility of the Ly α emission line during the EoR, and compute the total fraction of emitted Ly α photons that the IGM transmits directly to the observer, $\overline{\mathcal{T}}_{\text{IGM}}$. We simultaneously include the inhomogeneous large-scale reionization morphology, peculiar velocity offsets of the galaxies and IGM, and radiative transfer through the galactic outflows that is calibrated by observations of Lyman Alpha Emitters (LAEs) at $z < 6$ (Verhamme et al. 2006, 2008; Vanzella et al. 2010). This, in combination with the fact that we compute the full $\overline{\mathcal{T}}_{\text{IGM}}$ -PDF, clearly distinguishes our analysis from previous work.

Our models do not include dust, which at the redshifts of interest ($z = 7 - 9$) is likely a good approximation (Stanway et al. 2005; Bouwens et al. 2010b; Hayes et al. 2011; Blanc et al. 2011). The dust opacity to Ly α photons inside galaxies is expected to increase towards lower redshift, as the cumulative dust content of the Universe increased with cosmic time. This expected evolution has a different sign than the IGM opacity which decreases towards lower redshift. Thus, our discussion regarding the redshift evolution of the IGM opacity is likely conservative.

The outline of this paper is as follows: in § 2, we describe our models for galactic outflows (§2.1) and IGM opacity (§2.2). In § 3 we present the corresponding Ly α transmission fractions. Within this context, we interpret the observations of Ly α emitting galaxies at $z > 6$ in § 4. We compare our results with previous work in § 5. Finally, we present our conclusions in § 6. We adopt the background cosmological parameters $(\Omega_{\Lambda}, \Omega_{\text{M}}, \Omega_b, n, \sigma_8, H_0) = (0.72, 0.28, 0.046, 0.96, 0.82, 70 \text{ km s}^{-1} \text{ Mpc}^{-1})$, matching the five-year results of the *WMAP* satellite (Komatsu et al. 2009). Unless stated otherwise, we quote all quantities in comoving units.

2 THE MODEL

As mentioned above, our model has two components: (i) the intrinsic Ly α line, which has been processed by Ly α scattering through galactic outflows, and (ii) the IGM opacity, which further processes the line through both resonant and damping wing absorption. We describe these below in turn.

¹ The peculiar velocity of a galaxy can also redshift Ly α photons away from resonance before they escape into the surrounding intergalactic medium (Cen et al. 2005). However, this redshift is typically significantly smaller than the redshift imparted by galactic outflows (see Dijkstra & Wyithe 2010).

2.1 Modeling Galactic Outflows

We employ the wind models described in Dijkstra & Wyithe (2010). In these models the outflow is represented by a spherically symmetric shell of HI gas that has a column density N_{HI} , and outflow velocity v_{wind} . The shell has a thickness of 0.1 kpc and a radius of 1.0 kpc (proper, also see Ahn et al. 2003). The outflow surrounds a central Ly α source which emits photons at line center. Since we focus solely on the total *fraction* of Ly α photons transmitted to the observer, the total Ly α luminosity of the source is irrelevant. A Monte-Carlo code (described in Dijkstra et al. 2006a) accurately follows the propagation of Ly α photons through the optically thick outflow. These models are very similar to the models that reproduce observed Ly α line profiles at $z = 3 - 5$ (Verhamme et al. 2006, 2008, see Dijkstra & Wyithe 2010 for a discussion of caveats etc.). In this paper, we focus on wind models with $N_{\text{HI}} = 10^{20} \text{ cm}^{-2}$ and $N_{\text{HI}} = 10^{21}$, and wind velocities of $v_{\text{wind}} = 25 \text{ km s}^{-1}$ and $v_{\text{wind}} = 200 \text{ km s}^{-1}$. For comparison, Verhamme et al (2008) reproduced observed Ly α line shapes for LAEs at $z < 5$ with $25 \text{ km/s} \leq v_{\text{wind}} \leq 400 \text{ km/s}$, and that $2 \times 10^{19} \text{ cm}^{-2} \leq N_{\text{HI}} \leq 7 \times 10^{20} \text{ cm}^{-2}$. Our fiducial model ($N_{\text{HI}} = 10^{20} \text{ cm}^{-2}$, $v_{\text{wind}} = 200 \text{ km s}^{-1}$) lies in the middle of this range.

The impact of galactic winds on the Ly α radiation field depends on the covering factor of the galactic outflow: for low covering factors only a small fraction of the emitted Ly α photons will be Doppler boosted to frequencies where the IGM opacity is reduced. The issue of the wind covering factor is therefore related to the overall impact of galactic winds on the Ly α radiation field. Existing observations (which extend out to $z \sim 6$) indicate that winds play an important role in the scattering process, implying a large covering factor of the outflowing scattering material (we discuss this further in § 5). Of course, it remains a possibility that winds properties, such as their covering factor, were different at $z > 6$. This would affect the impact of the (especially ionized) IGM on Ly α emission lines, and hence the observed redshift evolution of LAEs at these redshifts (see § 4.2).

2.2 Modeling the IGM Opacity

We use the publicly-available, semi-numerical code DexM² to generate evolved density, velocity, halo, and ionization fields at $z = 8.56$. This code and detailed tests are presented in Mesinger & Furlanetto (2007), Mesinger et al. (2010) and Zahn et al. (2010), to which we refer the reader for details. Here we briefly summarize our simulation.

Our simulation box is $L = 250 \text{ Mpc}$ on a side, with the final density, peculiar velocity, and ionization fields having grid cell sizes of 0.56 Mpc. Halos are filtered out of the 1800^3 linear density field using the excursion-set formalism, and then mapped to Eulerian coordinates at $z = 8.56$ through perturbation theory (Zeldovich 1970). Perturbation theory is also used to generate the evolved density and peculiar velocity fields. Corresponding ionization fields are created according to the excursion-set prescription described in Mesinger & Furlanetto (2007), with the modification from

² <http://www.astro.princeton.edu/~mesinger/Sim.html>

Zahn et al. (2010) to account for partially ionized cells. This prescription compares the number of ionizing photons produced in a region of a given scale to the number of neutral hydrogen atoms inside that region. We generate a suite of ionization fields at various values of \bar{x}_{HI} by varying the ionization efficiency of sources assumed to be hosted by atomically-cooled halos, with masses of $M_{\text{halo}} > 10^8 M_{\odot}$. All of these fields have been extensively tested against hydrodynamical cosmological simulations, and good agreement was found well past the linear regime (Mesinger & Furlanetto 2007; Zahn et al. 2010; Mesinger et al. 2010).

We then extract $\sim 10^4$ line-of-sights (LOSs) centered on halos in the mass range, $10^{10} M_{\odot} < M_{\text{halo}} < 3 \times 10^{10} M_{\odot}$. This choice of host halo masses is motivated by the UV derived star formation rate (SFR) of 2-4 $M_{\odot} \text{ yr}^{-1}$ (Lehnert et al. 2010), which corresponds to a halo mass of $\sim 10^{10} M_{\odot}$ in the cosmological hydrodynamic simulations of Trac & Cen (2007)³. Opacities at wavelengths surrounding the Ly α line are computed for each LOS, integrating underneath a Voigt absorption profile (e.g. Rybicki & Lightman 1979), and including contribution from both the ionized and neutral IGM, out to distances of 200 Mpc away from the source. Inside HII regions, a residual HI fraction is computed assuming ionization equilibrium with an ionization rate of $\Gamma_{\text{HII}} = 0.5 \times 10^{-12} \text{ s}^{-1}$, in rough agreement with estimates obtained from the $z \sim 5\text{--}6$ Ly α forest (e.g., Fan et al. 2006; Bolton & Haehnelt 2007)⁴. We include the peculiar velocities of both the source halo and the absorbing gas, which can be very important (e.g. Dijkstra et al. 2007b; Iliev et al. 2008; Laursen et al. 2011).

3 RESULTS

To quantify the detectability of the Ly α line, we compute for each LOS the total fraction of emitted Ly α photons that

³ Our results are not sensitive to uncertainties of a factor of few in the host halo mass, because the halo bias evolves relatively slowly with mass in this range (Mesinger & Furlanetto 2008a; McQuinn et al. 2008; Mesinger & Furlanetto 2008b).

⁴ We emphasize that there is currently no evidence that reionization has completed at these redshifts (Lidz et al. 2007; Mesinger 2010; McGreer et al. (2011)). If the observed quasar spectra go through regions of pre-overlap neutral gas, the inferred value of a homogeneous Γ_{tot} would include contributions from the neutral IGM ($\Gamma \sim 0$). Therefore, the derived values of Γ_{tot} (from, e.g., Fan et al. 2006; Bolton & Haehnelt 2007) can be treated as lower limits for the ionization rate *inside the ionized component of the IGM*, Γ_{HII} .

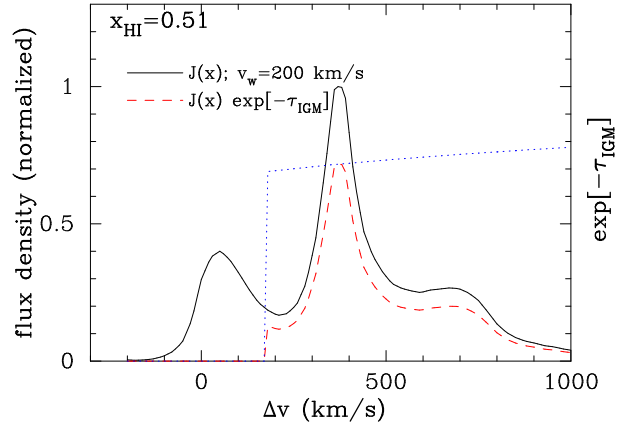


Figure 1. This Figure shows an example of a Ly α line profile. The *solid line* shows the Ly α spectrum—in units of the peak flux density—that emerges from the galaxy after the photons have scattered through the HI outflow. The *blue dotted line* shows the IGM opacity, $\exp[-\tau_{\text{IGM}}(\nu)]$ as a function of velocity offset Δv for $\bar{x}_{\text{HI}} = 0.51$. The *red dashed line* shows the spectrum of photons after processing the IGM, i.e. $J(\nu) \exp[-\tau_{\text{IGM}}(\nu)]$. This Figure nicely shows the impact of resonant scattering in the ionized IGM at $\Delta v \lesssim 170 \text{ km s}^{-1}$, and the impact of the damping wing optical depth at $\Delta v \gtrsim 170 \text{ km s}^{-1}$. The latter varies only weakly with frequency.

the IGM transmits directly to the observer, \mathcal{T}_{IGM} , as⁵

$$\mathcal{T}_{\text{IGM}} = \int_{\nu_{\text{min}}}^{\nu_{\text{max}}} d\nu J(\nu) \exp[-\tau_{\text{IGM}}(\nu)], \quad (1)$$

where $\tau_{\text{IGM}}(\nu)$ is the optical depth of the intervening IGM at frequency ν (computed as described in §2.2), and $J(\nu)$ is the normalized (i.e. $\int J(\nu) d\nu = 1$) Ly α spectrum of Ly α photons that emerges from the galaxy (computed as described in §2.1). The integral runs from $\sim 10^3 \text{ km s}^{-1}$ blueward to $\sim 3 \times 10^3 \text{ km s}^{-1}$ redward of the Ly α line resonance, which spans the full range of velocities that is covered by the Ly α profile that emerges from the galaxy. The quantity \mathcal{T}_{IGM} is also referred to as the ‘IGM transmission fraction’.

3.1 An Example Line Profile

An example on an observed Ly α line profile is shown in Figure 1. In this plot, the *solid line* shows the Ly α spectrum—in units of the peak flux density—that emerges from the galaxy after the photons have scattered through the HI outflow (in this case $v_{\text{wind}} = 200 \text{ km s}^{-1}$, and $N_{\text{HI}} = 10^{20} \text{ cm}^{-2}$). Most of the line flux is systematically redshifted relative to the galaxy’s systemic velocity. The flux density peaks

⁵ Photons that are scattered in the neutral IGM produce diffuse Ly α halos around individual sources (e.g. Zheng et al. 2010b). This emission is several orders of magnitude fainter than the detection threshold of the deepest observations to date (see Dijkstra & Wyithe 2010). Ly α radiation that is resonantly scattered in close proximity ($\lesssim 10 \text{ kpc}$) to the galaxy can give rise to a brighter Ly α halos (Zheng et al. 2010a,b). However, winds reduce the brightness of these halos (Dijkstra & Wyithe 2010). In any case, by ignoring this resonantly scattered component, we underestimate the true Ly α flux that can be detected from galaxies during the EoR, which only renders our results conservative.

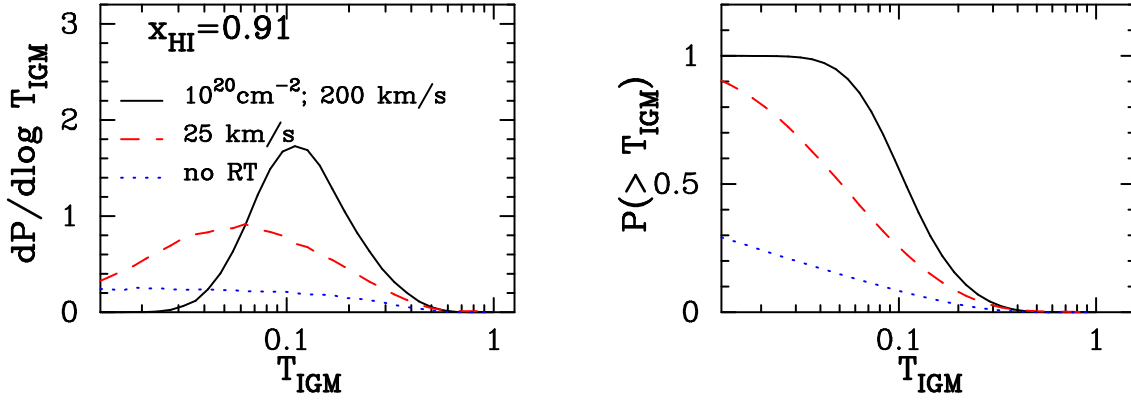


Figure 2. *Left panel:* This Figure shows the probability density, $\frac{dP}{d\log T_{\text{IGM}}}$, that the IGM transmits to the observer a fraction of emitted Ly α photons in the range $\log T_{\text{IGM}} \pm d\log T_{\text{IGM}}/2$, for galaxies populating dark matter halos of $10^{10} M_{\odot} < M_{\text{halo}} < 3 \times 10^{10} M_{\odot}$ in a universe with a neutral fraction of $\bar{x}_{\text{HI}} = 0.91$ (by volume) at $z = 8.6$. The red dashed line (black solid line) shows the model with $v_{\text{wind}} = 25$ (200) km s^{-1} . In both models $N_{\text{HI}} = 10^{20} \text{ cm}^{-2}$. The blue dotted line shows the ‘no-RT’ model (see text). This Figure illustrates that (i) the IGM can transmit a significant fraction of Ly α photons, despite the fact that reionization has only just started (text), and (ii) the IGM becomes even more ‘transparent’ when winds are affecting Ly α scattering in the ISM. *Right panel:* Same as the left panel, but now we plot the cumulative distribution function (CDF), $P(> T_{\text{IGM}})$. We find for example that $T_{\text{IGM}} > 10\%$ for $\sim 10\%$ of all halos in the ‘no-RT’ model, and that this fraction is boosted when winds are present.

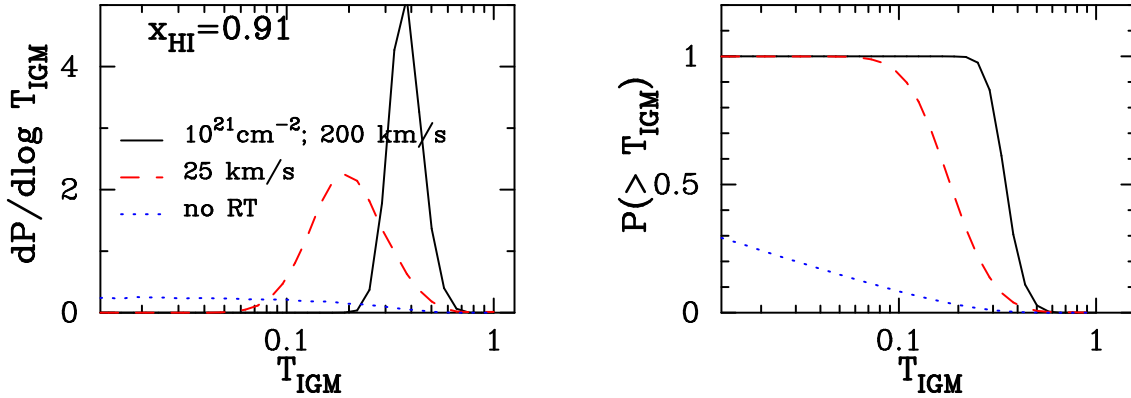


Figure 3. Same as Figure 2, but with an enhanced HI column density in the wind of $N_{\text{HI}} = 10^{21} \text{ cm}^{-2}$. Frequency diffusion that occurs as Ly α photons scatter through an extremely opaque medium causes a larger fraction of photons to emerge at larger redshifts from the line center, which reduces the effective IGM opacity.

at $\sim 2v_{\text{wind}}$, which is expected for radiation that scattered to the observer from the outflowing gas on the far side of the Ly α source (see Ahn et al. 2003; Verhamme et al. 2006; Dijkstra & Wyithe 2010).

The blue dotted line shows the IGM opacity, or more precisely $\exp[-\tau_{\text{IGM}}(\nu)]$ as a function of velocity off-set Δv for $\bar{x}_{\text{HI}} = 0.51$. In this particular example infalling (ionized) gas provides a large opacity to Ly α photons, even at velocities redward of the Ly α line center (in the frame of the galaxy, e.g. Santos 2004; Dijkstra et al. 2006b, 2007b; Iliev et al. 2008; Dayal et al. 2011; Zheng et al. 2010a; Laursen et al. 2011). That is, $\tau_{\text{IGM}} \gg 1$ at $\Delta v \lesssim +170 \text{ km s}^{-1}$. At redder wavelengths there is no gas that falls in fast enough for the Ly α photons to appear at resonance. At these frequencies ($\Delta v \gtrsim 170 \text{ km s}^{-1}$) the IGM opacity is dominated by the damping wing optical depth of the neutral IGM which is a smooth function of frequency.

The red dashed line shows the spectrum of photons after processing the flux through the IGM, i.e. $J(\nu) \exp[-\tau_{\text{IGM}}(\nu)]$. For this particular example, a fraction

$T_{\text{IGM}} = 0.57$ of all photons is transmitted directly to the observer. For comparison, had we assumed that all photons emerged from the galaxy with a Gaussian emission line, centered on the galaxy’s systemic velocity and with a standard deviation of $\sigma = v_{\text{circ}} \sim 80 \text{ km s}^{-1}$, we would have found that $T_{\text{IGM}} = 0.01$.

3.2 The Probability Distribution Function (PDF) of T_{IGM}

In Figure 2, we show the PDF, $\frac{dP}{d\log T_{\text{IGM}}}$ (left panel), and the cumulative distribution function (CDF), $P(> T_{\text{IGM}})$ (right panel), for $\bar{x}_{\text{HI}} = 0.91$. The red dashed lines (black solid lines) correspond to models with $v_{\text{wind}} = 25$ (200) km s^{-1} , and $N_{\text{HI}} = 10^{20} \text{ cm}^{-2}$ (both models). For the low (high) wind velocity we find that the $\log T_{\text{IGM}}$ -PDF peaks around ~ 0.06 (0.1). Increasing the wind velocity clearly shifts the T_{IGM} -PDF to larger values. As the Ly α photons scatter off of the receding outflows, they are Doppler shifted to larger effective redshifts (e.g., Ahn et al. 2003, Verhamme et al.

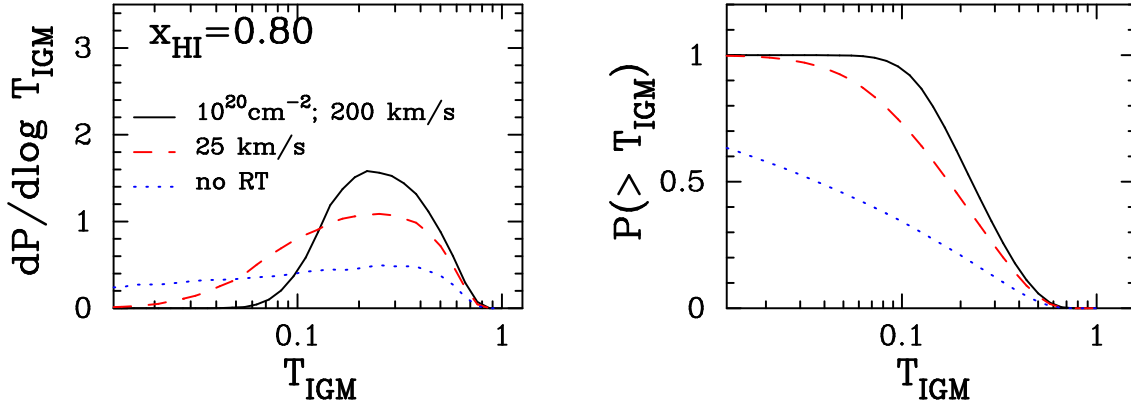


Figure 4. Same as Figure 2, but with a reduced global neutral hydrogen fraction, $\bar{x}_{\text{HI}} = 0.80$. The shifts of the \mathcal{T}_{IGM} -PDFs are due to the reduced neutral hydrogen content of the Universe.

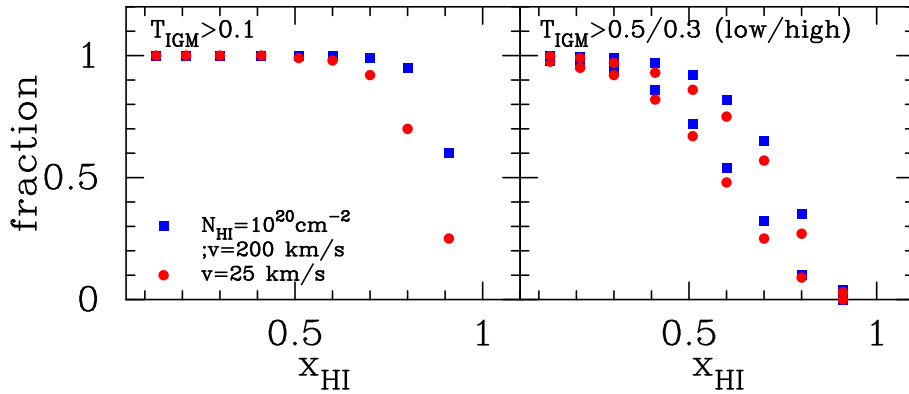


Figure 5. *Left panel:* The fraction of halos with $10^{10} M_{\odot} < M_{\text{halo}} < 3 \times 10^{10} M_{\odot}$ for which $\mathcal{T}_{\text{IGM}} > 0.1$ as a function of \bar{x}_{HI} , assuming $v_{\text{wind}} = 25$ (200) km s^{-1} , denoted by *red filled circles* (*blue filled squares*). In both models $N_{\text{HI}} = 10^{20} \text{ cm}^{-2}$. *Right panel:* same as the *left panel*, but now we plot the fraction of halos for which $\mathcal{T}_{\text{IGM}} > 0.3$ (top set of points), and $\mathcal{T}_{\text{IGM}} > 0.5$ (bottom set of points). This panel shows that the fraction of halos with $\mathcal{T}_{\text{IGM}} > 0.3$ only becomes less than $\sim 10\%$ when $\bar{x}_{\text{HI}} \gtrsim 0.90$. We therefore conclude that the observed strength of the Ly α line in the $z = 8.56$ galaxy is not surprising, unless the Universe was more than 90% neutral.

2006). Therefore, larger wind velocities cause a larger fraction of Ly α photons to emerge at frequencies where they are immune to the opacity in the ionized infalling IGM (see Fig. 1). Furthermore, this Doppler-shifting from the winds means that by the time the Ly α photons reach a neutral patch of the IGM, their absorption cross-sections are further out on the damping wing tail. Therefore, outflows reduce the impact of both resonant and damping with opacities (see Fig 1). Specifically, the right panel shows that $\mathcal{T}_{\text{IGM}} > 10\%$ for $\sim 30\%$ ($\sim 60\%$) of LAEs for $v_{\text{wind}} = 25$ km s^{-1} ($v_{\text{wind}} = 200$ km s^{-1}).

To underline the effect of winds, we compare to a model in which we only evaluate the damping wing optical depth, τ_{D} at line center, i.e. we set $\mathcal{T}_{\text{IGM}} \equiv -\ln \tau_{\text{D}} (\Delta\nu = 0)$. This model is referred to as the ‘no-RT’ model, as it corresponds to a model in which no scattering of Ly α photons occurs in the either the ISM or the ionized IGM, and is represented by the *blue dotted line*. The \mathcal{T}_{IGM} is clearly skewed more to lower values for this no-RT (‘RT’ stands for radiative transfer) model. That is, without winds a neutral IGM dramatically attenuates the transmission of the Ly α line. Only $\sim 10\%$ of LAE have transmission fractions greater than 0.1 (as has been demonstrated repeatedly in the past, e.g., Cen & Haiman 2000, Santos 2004; Furlanetto et al.

2004; McQuinn et al. 2008; Mesinger & Furlanetto 2008a,b). Winds therefore clearly boost the detectability of Ly α emission from galaxies during the early phases in the EoR.

Figure 3 shows the same quantities as Figure 2, but for wind models with $N_{\text{HI}} = 10^{21} \text{ cm}^{-2}$. The ‘no-RT’ model is of course unchanged. The \mathcal{T}_{IGM} -PDFs are shifted to larger values, because resonant scattering through very opaque media (the line-center optical depth to Ly α photons is $\tau_0 = 5.9 \times 10^7 (N_{\text{HI}}/10^{21} \text{ cm}^{-2})(T_{\text{gas}}/10^4 \text{ K})^{-1/2}$), results in frequency diffusion which increases with optical depth τ_0 (e.g. Harrington 1973, Neufeld 1990). As a result of this frequency diffusion, a larger fraction of photons will emerge at larger redshifts from the line center, which further reduces the effective IGM opacity.

Figure 4 shows the same as Figure 2, but for a lower volume averaged neutral fraction of $\bar{x}_{\text{HI}} = 0.80$. We find that $\mathcal{T}_{\text{IGM}} > 10\%$ for $\sim 35\%$ for the no-RT model, and that $\mathcal{T}_{\text{IGM}} > 10\%$ for $\sim 75\%$ ($\sim 95\%$) of all halos for the wind model with $v_{\text{wind}} = 25$ km s^{-1} ($v_{\text{wind}} = 200$ km s^{-1}). This shift of the \mathcal{T}_{IGM} -PDF arises because of the reduced neutral hydrogen content of the Universe.

4 COMPARISON TO RECENT DATA

4.1 Interpretation of the Recent Observations of a $z = 8.56$ Galaxy

The observed Ly α luminosity of the $z = 8.56$ galaxy is $L_\alpha = [5.5 \pm 1.0 \pm 1.8] \times 10^{42}$ erg s $^{-1}$ (the first number denotes the $1 - \sigma$ -uncertainty, while the second denotes the systematic uncertainty), while the UV luminosity density is $L_\nu(\lambda = 1700 \text{ \AA}) = 10^{28.3 \pm 0.2}$ erg s $^{-1}$ Hz $^{-1}$ at $\lambda = 1700 \text{ \AA}$ (rest-frame, Lehnert et al. 2010). From these observed strengths of the line and continuum, we can constrain the observed Ly α rest frame equivalent width (REW) to be (Dijkstra & Westra 2010):

$$\begin{aligned} \text{REW} &= \frac{L_\alpha}{L_\lambda(\lambda = \lambda_\alpha)} = \frac{\lambda_\alpha}{\nu_\alpha} \frac{L_\alpha}{L_\nu(\lambda = \lambda_\alpha)} = \\ &= \frac{\lambda_\alpha}{\nu_\alpha} \frac{L_\alpha}{L_\nu(\lambda = 1700 \text{ \AA})} \left(\frac{1216}{1700} \right)^{\beta-2} = 136^{+88}_{-55} \pm 45 \text{ \AA}. \end{aligned} \quad (2)$$

We assumed that the UV continuum slope is $\beta = 2$, which is appropriate for star forming galaxies with strong Ly α emission at $z = 3-7$ (Stark et al. 2010a). Bouwens et al. (2010b) determined $\beta \sim 3$ for candidate $z \sim 7$ (z_{850} drop-out) galaxies, with $M_{\text{UV}} \sim -19$ to ~ -18 . Inserting $\beta = 3$ into Eq 2 reduces the expectation value for REW to REW = 97 \AA.

The quoted $1 - \sigma$ uncertainty on REW is dominated by the uncertainty in the observed UV flux density. The uncertainty on the observed REW is large, but the expectation value is remarkably large (even for $\beta = 3$). The intrinsic Ly α REW, REW $_{\text{int}}$, depends quite strongly on gas metallicity, and whether the galaxy is forming stars in a burst or continuously (e.g. Fig 7 of Schaerer 2003), and whether the ‘case-B’ approximation is valid (Raiter et al. 2010). The maximum possible value appears to be REW $_{\text{max}} = 3000 \text{ \AA}$ (Raiter et al. 2010). This maximum value is reached if this galaxy formed stars from metal-free gas in a burst with a top-heavy initial mass function. Under this assumption, the data requires that the IGM transmits $\mathcal{T}_{\text{IGM}} \sim 0.04^{+0.03}_{-0.02} \times \left(\frac{\text{REW}_{\text{int}}}{3000 \text{ \AA}} \right)^{-1}$, where REW $_{\text{int}}$ denotes the intrinsic (or emitted) REW. In theory, we could explain the observed REW for $\mathcal{T}_{\text{IGM}} \gtrsim 0.04^{+0.03}_{-0.02}$. However, throughout we focus on the more conservative requirement $\mathcal{T}_{\text{IGM}} > 0.1$, which requires smaller values for the intrinsic REW.

For comparison, Figures 2-4 show that even with low velocity outflows ($v_{\text{wind}} = 25 \text{ km s}^{-1}$) $\mathcal{T}_{\text{IGM}} > 0.1$ for a significant fraction LAEs, even if the Universe is $\sim 91\%$ neutral. This is illustrated more explicitly in Figure 5, where the *left panel* shows the fraction of LAEs for which $\mathcal{T}_{\text{IGM}} > 0.1$ as a function of \bar{x}_{HI} for $v_{\text{wind}} = 25$ (200) km s $^{-1}$ as *red filled circles* (*blue filled squares*), where $N_{\text{HI}} = 10^{20} \text{ cm}^{-2}$ in both models. This fraction is $\gtrsim 50\%$ for both models when $\bar{x}_{\text{HI}} \lesssim 80\%$. The *right panel* is the same as the *left panel*, but for $\mathcal{T}_{\text{IGM}} > 0.3$ (upper set of points), and $\mathcal{T}_{\text{IGM}} > 0.5$ (lower set of points). This panel shows that the fraction of LAEs with $\mathcal{T}_{\text{IGM}} > 0.3$ only becomes less than $\sim 10\%$ when $\bar{x}_{\text{HI}} \gtrsim 0.80$. We therefore conclude that the strength of the Ly α line of the $z = 8.56$ galaxy is not surprising, unless the Universe were more than 90% neutral by volume.

This latter statement is quantified in Figure 6, where we plot the conditional probability distribution for \bar{x}_{HI} , if we require that $\mathcal{T}_{\text{IGM}} > 0.1$ (the three lines represent the same models that were shown in Fig 2-4).

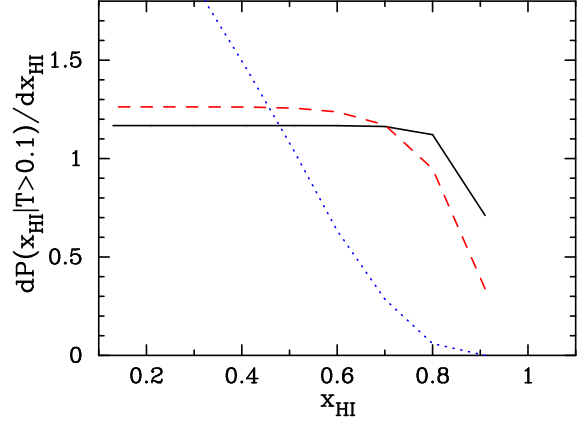


Figure 6. This figure shows the marginalized PDF for \bar{x}_{HI} , given that $\mathcal{T}_{\text{IGM}} > 0.1$, denoted by $\frac{dP(\bar{x}_{\text{HI}}|\mathcal{T}_{\text{IGM}}>0.1)}{d\bar{x}_{\text{HI}}}$. Different lines represent the different models that were also shown in Figures 2-4. This Figure shows clearly that it is difficult to rule out even large values of \bar{x}_{HI} with confidence—especially when winds are included in the modeling (see text).

This PDF follows from Bayes theorem as⁶ $p(\bar{x}_{\text{HI}}|\mathcal{T}_{\text{IGM}}) = p(\mathcal{T}_{\text{IGM}}|\bar{x}_{\text{HI}})p_{\text{prior}}(\bar{x}_{\text{HI}})/p(\mathcal{T}_{\text{IGM}})$. We explicitly computed the term $\frac{dP(\mathcal{T}_{\text{IGM}}|\bar{x}_{\text{HI}})}{d \log \mathcal{T}_{\text{IGM}}} = \ln 10 \times \mathcal{T}_{\text{IGM}} \times p(\mathcal{T}_{\text{IGM}}|\bar{x}_{\text{HI}})$ in this paper. Examples were shown in Figure 2 ($\bar{x}_{\text{HI}} = 0.91$) and Figure 4 ($\bar{x}_{\text{HI}} = 0.80$). The term $p_{\text{prior}}(\bar{x}_{\text{HI}})$ is the prior probability distribution for \bar{x}_{HI} , which we assumed to be flat. This expression only gives us the conditional PDF for \bar{x}_{HI} for a given value of \mathcal{T}_{IGM} . To get a marginalized PDF, we compute $p(\bar{x}_{\text{HI}}|\mathcal{T}_{\text{IGM}} > 0.1) = \int_{0.1}^{1.0} p(\bar{x}_{\text{HI}}|\mathcal{T}_{\text{IGM}})p(\mathcal{T}_{\text{IGM}})d\mathcal{T}_{\text{IGM}}$, which simplifies to $p(\bar{x}_{\text{HI}}|\mathcal{T}_{\text{IGM}} > 0.1) = \int_{0.1}^{1.0} p(\mathcal{T}_{\text{IGM}}|\bar{x}_{\text{HI}})d\mathcal{T}_{\text{IGM}}$ (for our assumption that $p_{\text{prior}}(\bar{x}_{\text{HI}}) = 1$).

If we require that $\mathcal{T}_{\text{IGM}} > 0.1$, then the *blue dotted line* shows that for the model without winds, a low neutral fraction is preferred. However, the statistical significance of this statement is weak: for this model $\bar{x}_{\text{HI}} < 0.70$ at $\sim 95\%$ CL. Once winds are included, this constraint becomes even weaker, and it is not even possible to ‘strongly’ (i.e. $> 95\%$ CL) rule out⁷ $\bar{x}_{\text{HI}} \geq 0.91$. We caution against interpreting these numbers literally, as the overall shape of the PDF is completely dominated by the assumed prior on \bar{x}_{HI} . This illustrates that it is difficult to rule out even large values of \bar{x}_{HI} with confidence—especially when winds are included in the modeling.

4.2 Interpreting the Apparent Fast Drop in the ‘LAE Fraction’ among LBGs

Stark et al. (2010a) recently found that the fraction of drop-

⁶ Note that we switched to the shorter notation from probability theory, and denote probability density functions by $p(a) \equiv \frac{dP(a)}{da}$, and conditional PDFs by $p(a|b) \equiv \frac{dP(a|b)}{da}$.

⁷ If we require that $\mathcal{T}_{\text{IGM}} > 0.3$, then we can rule out $\bar{x}_{\text{HI}} \geq 0.80$ at $\sim 95\%$ CL for both wind models. Given existing uncertainties on both observed and intrinsic REW of the Ly α line, requiring the IGM to transmit more than 30% is not well motivated. We therefore consider any constraints on \bar{x}_{HI} from this requirement not relevant.

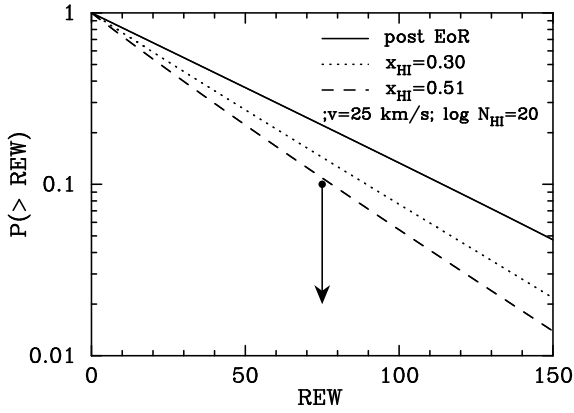


Figure 7. We show the CDF for REW. The *solid line* shows an exponential Ly α REW-distribution that represents a simplified representation of the $z = 6$ drop-out population (see text). The *dashed line* [*dotted line*] shows the $z = 7$ PDF under the assumption that the observed LAE fraction at $z = 7$ is different only because of the IGM, that the Universe was 51% [30%] neutral by volume (i.e. $\bar{x}_{\text{HI}} = 0.51$ [$\bar{x}_{\text{HI}} = 0.30$]), and for the wind model with $(N_{\text{HI}}, v_{\text{wind}}) = (10^{20} \text{ cm}^{-2}, 25 \text{ km s}^{-1})$. We also show the upper limit that was derived by Stark et al. (2010a, 2011) for $z = 7$ drop-out galaxies. Explaining the observed rapid change in the LAE fraction among the drop-out population with reionization would require a fast evolution of the neutral fraction of hydrogen in the Universe.

out galaxies with strong Ly α emission decreases strongly from $z = 6$ to $z = 7$ (also see Stark et al. 2011). More specifically, they found that the fraction of drop-out galaxies with a $\text{REW} \gtrsim 75 \text{ \AA}$ Ly α line decreased by a factor of ~ 2 between $z = 6$ and $z = 7$. A similar observation was made by Fontana et al. (2010), who detected (weak; $\text{REW} \sim 13 \text{ \AA}$) Ly α emission in only 1 out of 7 candidate $z = 7$ drop-out galaxies. These trends are not seen at $z \lesssim 6$. Such a sudden, strong suppression of Ly α flux from galaxies at $z = 7$ could be a signature related to reionization, although the available data still has large uncertainties. The Stark et al. (2010a, 2011) sample is consistent with no redshift evolution between $z = 6$ and $z = 7$ at the $\sim 1 \sigma$ level. And the statistical significance of the drop observed by Fontana et al. (2010) implicitly relies on the assumption that all seven drop-out galaxies are indeed at $z \sim 7$. Nevertheless, it is an interesting exercise to interpret these observations as is.

In this work, we computed the \mathcal{T}_{IGM} -PDF at various ionization stages of the IGM during the EoR. Suppose that the observed REW-distribution at $z = 6$ is described by an exponential function (which provides a good fit to observed LAEs at $z = 2-4$, see Gronwall et al. 2007, Blanc et al. 2011) between $\text{REW} = 0$ and $\text{REW} = 300 \text{ \AA}$, i.e. $P_{z=6}(\text{REW}) \propto \exp[-\text{REW}/\text{REW}_c]$. If we choose a scalelength of $\text{REW}_c = 50 \text{ \AA}$, then the fraction of drop-out galaxies with $\text{REW} \gtrsim 75 \text{ \AA}$ is $f \sim 0.2$, which corresponds to the median value observed by Stark et al. (2010a) at $z \sim 6$.

We now conservatively assume that the IGM at $z = 6$ was 100% transparent to Ly α photons emitted by galaxies, and that the observed REW-PDF at $z = 7$ is different only because of evolution of the ionization state of the IGM. Under this assumption, an observed REW at $z = 7$ requires an intrinsic (i.e. emitted) equivalent width of $\text{REW}/\mathcal{T}_{\text{IGM}}$, and we can compute the observed REW-PDF at $z = 7$

as $P_{z=7}(\text{REW}) = \mathcal{N} \int_0^1 d\mathcal{T}_{\text{IGM}} P(\mathcal{T}_{\text{IGM}}) P_{z=6}(\text{REW}/\mathcal{T}_{\text{IGM}})$. Here, $P(\mathcal{T}_{\text{IGM}})$ denotes the \mathcal{T}_{IGM} -PDF computed in this paper. The equation sums over all possible \mathcal{T}_{IGM} with the proper probabilities that a galaxy had a Ly α line with $\text{REW}/\mathcal{T}_{\text{IGM}}$ and that the IGM transmitted a fraction \mathcal{T}_{IGM} . Finally, the factor \mathcal{N} normalizes $P_{z=7}(\text{REW})$.

Figure 7 shows our model CDF of REW for $z = 6$ drop-out galaxies as the *solid line*, and for $z = 7$ drop out galaxies⁸ $\bar{x}_{\text{HI}} = 0.51$ ($\bar{x}_{\text{HI}} = 0.30$) as the *dashed line* (*dotted line*). We used the wind model with $(N_{\text{HI}}, v_{\text{wind}}) = (10^{20} \text{ cm}^{-2}, 25 \text{ km s}^{-1})$.

Stark et al. (2010a, 2011) put the upper limit on the fraction of drop-out galaxies with Ly α $\text{REW} \gtrsim 75 \text{ \AA}$ at $\lesssim 0.10$ (also shown in Fig 7). The plots show that in order to explain the observed evolution between $z = 6$ and $z = 7$, we require a rapid evolution of the neutral fraction of hydrogen in the Universe (i.e. $\Delta\bar{x}_{\text{HI}} \sim 0.5$ over $\Delta z = 1$)⁹. We stress that we assumed that $\mathcal{T}_{\text{IGM}} = 1$ at $z = 6$. If we had instead used a \mathcal{T}_{IGM} -PDF appropriate for a fully ionized medium at $z = 6$, then we would have needed the IGM at $z = 7$ to be even more opaque, which required an even faster evolution in \bar{x}_{HI} . As we mentioned already in § 1, dust (as well as evolution in metallicity) would also require a faster evolution in \bar{x}_{HI} . For larger wind velocities and/or HI column densities, we would again need a larger volume fraction of HI. Additionally, the data of Fontana et al. (2010) implies an even stronger evolution in the observed REW-PDF, and hence in the overall neutral fraction.

Theoretically, the above-inferred rapid redshift evolution in \bar{x}_{HI} is unrealistic even in models with no negative feedback on the source population (e.g., Barkana & Loeb 2001; Fig. 9 in Mesinger et al. 2006; Fig. 1 in Lidz et al. 2007). Furthermore, the sinks of ionizing photons (Lyman limit absorption systems) likely further slow the final stages of reionization (e.g., Furlanetto & Mesinger 2009; Alvarez & Abel 2010; Crociani et al. 2011), whose photoevaporation timescales could be much longer than $\Delta z \sim 1$ (Iliev et al. 2005). The inferred rapid evolution could mean that the current sample of $z = 7$ drop-out galaxies trace a region of the Universe that was more neutral than average. Alternatively, it could signal other physical effects: for example, a decreasing wind strength or covering factor towards higher redshifts can enhance the impact of the ionized IGM, and

⁸ Of course, we computed the \mathcal{T}_{IGM} -PDF at $z = 8.6$, and now apply our models to $z = 7$ data. As a result, our model overestimates the Gunn-Peterson optical depth. We therefore overestimated the damping wing opacity of the neutral IGM. If we had included the proper damping wing optical depth (i.e. at the correct redshift), we would again have required an even larger \bar{x}_{HI} to obtain the same total optical depth. Our current inferred rate of the evolution of \bar{x}_{HI} is therefore conservative.

⁹ Our constraint on the redshift-evolution in \bar{x}_{HI} depends somewhat on the assumed range over which exponential function provides a good fit to the data. For example, under the extreme assumption that there were no drop-out galaxies at $z = 6$ with $\text{REW} \leq 20 \text{ \AA}$, then we would need a scalelength of $\text{REW}_c \sim 40 \text{ \AA}$ to be consistent with Stark et al. (2010a). In this case, we would ‘only’ require that $\Delta\bar{x}_{\text{HI}} \sim 0.3$ over $\Delta z = 1$. However Stanway et al. (2007) found that the fraction of drop-out galaxies with weak emission ($\text{REW} \lesssim 25 \text{ \AA}$) is consistent with the observed fraction at $z = 3$, which suggests that this ‘extreme’ model is unrealistic.

thus increase the rate at which the IGM opacity changes. Yet another interesting possibility is that the observed rapid evolution in the Ly α REW-PDF of the drop-out galaxy population is entirely due to reionization, but that the Universe at $z = 6$ still contained a non-negligible volume fraction of neutral hydrogen (for a discussion on the current observational constraints, see Mesinger 2010 and McGreer et al., 2011). This is because the fraction of galaxies for which $\mathcal{T}_{\text{IGM}} > 0.3$ (as an example) evolves more rapidly at $\bar{x}_{\text{HI}} \gtrsim 0.5$ (i.e. $df/d\bar{x}_{\text{HI}}$ is largest when $\bar{x}_{\text{HI}} \sim 0.5$; see Fig 5). For example, the fraction of galaxies with $\mathcal{T}_{\text{IGM}} > 0.3$ changes more rapidly between $\bar{x}_{\text{HI}} = 0.5$ and $\bar{x}_{\text{HI}} = 0.7$, then between $\bar{x}_{\text{HI}} = 0.0$ and $\bar{x}_{\text{HI}} = 0.5$ (see Fig 5). This scenario however would require an extended early epoch of reionization to be consistent with WMAP observations, perhaps driven by negative feedback on smaller-mass sources. Clearly it will be important to constrain the evolution of the LAE fraction between $z = 6$ and $z = 7$ with a larger sample of galaxies.

Finally, we point out that the observed drop in the LAE fraction between $z = 6$ and $z = 7$ is consistent with observations of the LAE populations at $z = 5.7$ and $z = 6.5$. The Ly α luminosity function of LAEs evolves significantly between $z = 6.5$ and $z = 5.7$ (Shimasaku et al. 2006; Kashikawa et al. 2006; Ouchi et al. 2010). However, the rest-frame UV luminosity function of these same galaxies does not evolve between these redshifts (Kashikawa et al. 2006). Dijkstra et al. (2007a) showed that these two observations combined translate to a reduction in the number of detected Ly α photons from $z = 6.5$ by a factor of 1.1–1.8 (95% CL) relative to $z = 5.7$, with a median value of ~ 1.3 (Ouchi et al. 2010). Hu et al. (2010) recently obtained spectroscopic observations of narrowband selected LAEs at $z = 5.7$ and $z = 6.5$ and found that the Ly α REW of the average $z = 5.7$ [$z = 6.5$] spectrum was $\text{REW} \sim 34 \pm 2 \text{ \AA}$ [$\text{REW} \sim 23 \pm 3 \text{ \AA}$]. This corresponds to a reduction in the number of detected Ly α photons from $z = 6.5$ by a factor of ~ 1.3 relative to $z = 5.7$, consistent with the value inferred from the redshift evolution of the luminosity functions. This provides evidence for evolution in the REW-PDF that is similar to the trends seen in the drop-out population by Stark et al. (2010a) and Fontana et al. (2010).

5 COMPARISON TO PREVIOUS WORK

We found that $\mathcal{T}_{\text{IGM}} \gtrsim 50\%$ for the majority of galaxies, even when the Universe is $\sim 60\%$ neutral by volume. In our models, the IGM is more transparent than in previous studies of the visibility of LAEs during the EoR. Mesinger & Furlanetto (2008b) assumed a constant opacity in the ionized IGM, and only considered velocity offsets in the Ly α line due to the peculiar velocities of the dark matter halos (which are much smaller than the velocity offsets that can be imparted by winds). McQuinn et al. (2007) studied a very similar model, but did not include the halos’ peculiar velocities. McQuinn et al. (2007) also investigated a ‘wind model’ in which the Ly α line was redshifted by 400 km s^{-1} , and found a considerable boost in the IGM transmission fraction for $\bar{x}_{\text{HI}} \gtrsim 0.7$ (see their Figure 6). Iliev et al. (2008) studied the impact of the ionized IGM on the Ly α line profile in more detail, but assumed Gaussian emission lines, which can reduce the IGM transmission factor significantly compared to

models that include outflows (see § 3.1 for a clear illustration of this effect).

Perhaps surprisingly, our quoted values for \mathcal{T}_{IGM} are significantly higher than the values quoted in previous works *even for a fully ionized IGM*. For example, Dijkstra et al. (2007b) found that the ionized IGM could transmit as little as $\mathcal{T}_{\text{IGM}} = 0.1\text{--}0.3$ at $z > 4.5$ for a fully ionized IGM (also see Dayal et al. 2010). Laursen et al. (2011) recently constrained $\mathcal{T}_{\text{IGM}} = 0.26^{+0.13}_{-0.18}$ at $z = 5.7$. Zheng et al. (2010a) find that $\mathcal{T}_{\text{IGM}} \sim 0.01\text{--}0.3$, which in detail depends on luminosity¹⁰.

The main difference between the present and previous work are due to outflows, which causes most of the line flux to be systematically redshifted relative to the galaxy’s systemic velocity (see § 3). We acknowledge that the outflow models were calibrated on the models of Verhamme et al. (2008) which assumed that the IGM at $z = 2\text{--}5$ had no impact on the observed Ly α line shapes. It is certainly possible—especially towards higher redshifts—to reproduce observed Ly α line shapes with ‘weaker’ (i.e. lower velocity) outflows once the IGM is included. This is illustrated by recent work of Laursen et al. (2011), who modeled Ly α RT in simulated, dusty galaxies. Laursen et al. (2011) found that Ly α photons emerge from their simulated galaxies with a broadened, double peaked profile (also see Barnes et al. 2011). The IGM at $z > 5$ cuts off the blue peak, which then results in a typically observed redshifted, asymmetric Ly α emission line (although at $z = 3.5$ the blue peak remains visible for a significant fraction of sightlines through the IGM). In these models, galactic outflows have little impact on the Ly α photons emerging from galaxies.

While it is likely that Ly α line shape is affected by the IGM to some extent (especially towards higher redshifts), outflows are also expected to play at least an important role. This is because outflows are ubiquitous in observed star forming galaxies, and the outflowing material has a large covering factor (Steidel et al. 2010). Importantly, there is evidence that outflows affect observed Ly α line spectra: (i) asymmetric line shapes are present at low redshift ($z \sim 0$), when the IGM should not have an impact (Mas-Hesse et al. 2003; Heckman et al. 2011); (ii) observations indicate that outflows promote the escape of Ly α from a dusty medium (Kunth et al. 1998; Atek et al. 2008); (iii) Schaerer & Verhamme (2008) and Dessauges-Zavadsky et al. (2010) successfully reproduced the Ly α spectrum of the Lyman Break galaxies cB58 and the ‘8 o’clock arc’ respectively, with outflow models very similar to our own and those by Verhamme et al. (2006, 2008), but whose parameters were constrained by low-ionization metal absorption lines. In these models, the wind parameters inferred from the Ly α line shape were consistent with those inferred from alternative observations. Steidel et al. (2010, 2011) also constructed a simple model for the Ly α

¹⁰ Note that Zheng et al. (2010a) include scattering inside the virial radius in their calculations, while for example Dijkstra et al. (2007b) and Laursen et al. (2011) do not. Gas within the virial radius can be significantly denser and can have larger peculiar velocities. This can explain that Zheng et al. (2010a) found lower values for \mathcal{T}_{IGM} . The fact that Zheng et al. (2010a) properly account for the possibility that photons scatter back into the LOS (in close proximity of the source) can only boost their \mathcal{T}_{IGM} compared to that of other groups, and cannot explain this difference.

spectra observed from LBGs—as well as the Ly α halos that are observed around LBGs—in which Ly α photons scatter primarily through a large-scale galactic outflow, whose structure is constrained by low-ionization metal absorption lines. Points (i–iii) underline the probable physical connection between the outflowing and scattering media.

We have shown that our main conclusions remain valid for wind velocities in excess¹¹ of $v_{\text{wind}} \gtrsim 25 \text{ km s}^{-1}$ (and $N_{\text{HI}} \geq 10^{20} \text{ cm}^{-2}$), which systematically redshifts the Ly α emission line as it emerges from a galaxy. We consider these requirements to be reasonable, given direct observational constraints on outflow velocities from low-ionization metal absorption lines (Steidel et al. 2010; Rakic et al. 2010), and on HI column density (as in cB58 and the ‘8 o’clock arc’, see e.g. Schaerer & Verhamme 2008 and Dessauges-Zavadsky et al. 2010),.

After the submission of this work, Dayal & Ferrara (2011, hereafter DF11) submitted a paper in which they constrained $\bar{x}_{\text{HI}} < 0.2$ using the same $z = 8.6$ galaxy. We argue that this upper limit is not robust for several reasons. Firstly, the model of DF11 does not include outflows. In contrast, we have summarized the strong observational evidence that galactic outflows affect the Ly α radiation field, implying that outflows must be included at some level in a realistic model. Secondly, there is an absence of large HII ‘bubbles’ in the model of DF11: the HII bubble radii in their model are $\lesssim 3 - 4 \text{ Mpc}$ when $\bar{x}_{\text{HI}} = 0.2$, while simulations of reionization that include radiative transfer of ionizing photons, show that the typical HII bubbles have radii that are a factor ~ 10 larger when $\bar{x}_{\text{HI}} \sim 0.3$ (see e.g. Fig 2 of Zahn et al. 2010). Our large scale semi-numeric simulations of reionization properly capture the bubble size distribution, and the fact that the more massive galaxies preferentially populate these large HII bubbles. This absence of large bubbles in the models of DF11 enhances the IGM opacity, which causes their constraints on \bar{x}_{HI} to be stronger than those obtained from our models where galactic winds are not included.

6 CONCLUSIONS

In this paper we have studied the visibility of the Ly α emission line during reionization. We combine large scale semi-numerical simulations of cosmic reionization with empirically-calibrated models of galactic outflows. With these sophisticated tools, we compute the PDFs of the IGM transmission fraction, \mathcal{T}_{IGM} . We find that winds cause $\mathcal{T}_{\text{IGM}} \gtrsim 10\%$ [50%], for the majority of galaxies, even when the Universe is $\sim 80\%$ [60%] neutral by volume. This only requires wind speeds greater than $\sim 25 \text{ km s}^{-1}$, which are quite conservative judging by the observed Ly α lines shapes at $z < 5$ (Verhamme et al. 2008, also see § 5). Therefore, we conclude that the observed strong Ly α emission from the reported $z = 8.6$ galaxy is consistent with a highly neutral IGM.

We also show that evoking reionization to explain the observed drop in the ‘LAE fraction’ (see § 4.2) of drop-out

galaxies between $z = 6$ and $z = 7$ (Stark et al. 2010a, 2011), requires a very rapid evolution of \mathcal{T}_{IGM} , corresponding to $\bar{x}_{\text{HI}} \sim 0 \rightarrow 0.5$ over $\Delta z = 1$. Reionization models find such a rapid evolution unrealistic, which may indicate that either (i) the current sample of drop-out galaxies at $z = 7$ happened to populate a region of our Universe that was more neutral than average, (ii) winds become weaker and/or have smaller covering factors towards higher redshifts, or (iii) that the Universe at $z = 6$ still contained a non-negligible volume fraction of neutral hydrogen. However, these conclusions are tentative as the available data still has large uncertainties.

Regardless of these current observational uncertainties, our work underlines the point that Ly α emission can be detected from galaxies in the earliest stages of reionization. This is a positive result for (narrowband) searches for high redshift Ly α emitters such as the ‘Emission-Line galaxies with VISTA Survey’ (ELVIS) (e.g. Nilsson et al. 2007). On the other hand, if a neutral IGM is quite transparent to Ly α photons, then a signature of reionization may be more difficult to extract from observations of Ly α emitting galaxies. However, the *redshift evolution* of quantities such as (i) the ‘LAE fraction’—or more generally the Ly α restframe equivalent width PDF—among LBGs (Stark et al. 2010a; Fontana et al. 2010; Stark et al. 2011), and (ii) the UV and Ly α luminosity functions of LAEs (Kashikawa et al. 2006), already provide interesting and useful constraints on models of reionization. Furthermore, the clustering signature of LAEs (McQuinn et al. 2007; Mesinger & Furlanetto 2008b, though see Iliev et al. 2008) is also affected by reionization, and it has already been shown that winds do not affect this prediction (McQuinn et al. 2007).

Acknowledgements Support for this work was provided by NASA through Hubble Fellowship grant HST-HF-51245.01-A to AM, awarded by the Space Telescope Science Institute, which is operated by the Association of Universities for Research in Astronomy, Inc., for NASA, under contract NAS 5-26555.

REFERENCES

- Ahn, S.-H., Lee, H.-W., & Lee, H. M. 2003, MNRAS, 340, 863
- Alvarez, M. A., & Abel, T. 2010, arXiv:1003.6132
- Atek, H., Kunth, D., Hayes, M., Östlin, G., & Mas-Hesse, J. M. 2008, A&A, 488, 491
- Atek, H., Schaerer, D., & Kunth, D. 2009, A&A, 502, 791
- Barkana, R., & Loeb, A. 2001, Physics Reports, 349, 125
- Barnes, L. A., Haehnelt, M. G., Tescari, E., & Viel, M. 2011, arXiv:1101.3319
- Blanc, G. A., et al. 2011, submitted to ApJ, arXiv:1011.0430
- Bolton, J. S., & Haehnelt, M. G. 2007, MNRAS, 382, 325
- Bouwens, R. J., et al. 2010a, ApJ, 709, L133
- Bouwens, R. J., et al. 2010b, ApJ, 708, L69
- Bunker, A. J., et al. 2010, MNRAS, 409, 855
- Cen, R., & Haiman, Z. 2000, ApJ, 542, L75
- Cen, R., Haiman, Z., & Mesinger, A. 2005, ApJ, 621, 89

¹¹ If we lower N_{HI} by an order of magnitude, then our main conclusions are unaffected provided that $v_{\text{wind}} \gtrsim 200 \text{ km s}^{-1}$. These requirements are also reasonable.

- Crociani, D., Mesinger, A., Moscardini, L., & Furlanetto, S. 2011, *MNRAS*, 411, 289
- Dayal, P., Maselli, A., & Ferrara, A. 2011, *MNRAS*, 410, 830
- Dayal, P., & Ferrara, A. 2011, arXiv:1102.1726
- Dessauges-Zavadsky, M., D’Odorico, S., Schaerer, D., Modigliani, A., Tapken, C., & Vernet, J. 2010, *A&A*, 510, A26
- Dijkstra, M., Haiman, Z., & Spaans, M. 2006a, *ApJ*, 649, 14
- Dijkstra, M., Haiman, Z., & Spaans, M. 2006b, *ApJ*, 649, 37
- Dijkstra, M., Wyithe, J. S. B., & Haiman, Z. 2007a, *MNRAS*, 379, 253
- Dijkstra, M., Lidz, A., & Wyithe, J. S. B. 2007b, *MNRAS*, 377, 1175
- Dijkstra, M., & Wyithe, J. S. B. 2010, *MNRAS*, 408, 352
- Dijkstra, M., & Westra, E. 2010, *MNRAS*, 401, 2343
- Fan, X., et al. 2006, *AJ*, 132, 117
- Finkelstein, S. L., Papovich, C., Giavalisco, M., Reddy, N. A., Ferguson, H. C., Koekemoer, A. M., & Dickinson, M. 2010, *ApJ*, 719, 1250
- Fontana, A., et al. 2010, *ApJ*, 725, L205
- Furlanetto, S. R., Zaldarriaga, M., & Hernquist, L. 2004, *ApJ*, 613, 1
- Furlanetto, S. R., & Mesinger, A. 2009, *MNRAS*, 394, 1667
- Gronwall, C., et al. 2007, *ApJ*, 667, 79
- Harrington, J. P. 1973, *MNRAS*, 162, 43
- Hayes, M., Schaerer, D., Östlin, G., Mas-Hesse, J. M., Atek, H., & Kunth, D. 2011, *ApJ*, 730, 8
- Heckman, T. M., et al. 2011, *ApJ*, 730, 5
- Hu, E. M., Cowie, L. L., Barger, A. J., Capak, P., Kakazu, Y., & Trouille, L. 2010, *ApJ*, 725, 394
- Iliev, I. T., Shapiro, P. R., & Raga, A. C. 2005, *MNRAS*, 361, 405
- Iliev, I. T., Shapiro, P. R., McDonald, P., Mellema, G., & Pen, U.-L. 2008, *MNRAS*, 391, 63
- Johnson, J. L., Greif, T. H., Bromm, V., Klessen, R. S., & Ippolito, J. 2009, *MNRAS*, 399, 37
- Kashikawa, N., et al. 2006, *ApJ*, 648, 7
- Komatsu, E., et al. 2009, *ApJS*, 180, 330
- Kunth, D., Mas-Hesse, J. M., Terlevich, E., Terlevich, R., Lequeux, J., & Fall, S. M. 1998, *A&A*, 334, 11
- Laursen, P., Sommer-Larsen, J., & Razoumov, A. O. 2011, *ApJ*, 728, 52
- Lehnert, M. D., et al. 2010, *Nature*, 467, 940
- Lidz, A., McQuinn, M., Zaldarriaga, M., Hernquist, L., & Dutta, S. 2007, *ApJ*, 670, 39
- Mas-Hesse, J. M., Kunth, D., Tenorio-Tagle, G., Leitherer, C., Terlevich, R. J., & Terlevich, E. 2003, *ApJ*, 598, 858
- McGreer, I. D., Mesinger, A., & Fan, X. 2011, submitted to *MNRAS*, arXiv:1101.3314
- McQuinn, M., Hernquist, L., Zaldarriaga, M., & Dutta, S. 2007, *MNRAS*, 381, 75
- McQuinn, M., Lidz, A., Zaldarriaga, M., Hernquist, L., & Dutta, S. 2008, *MNRAS*, 388, 1101
- Mesinger, A., Johnson, B. D., & Haiman, Z. 2006, *ApJ*, 637, 80
- Mesinger, A., & Furlanetto, S. 2007, *ApJ*, 669, 663
- Mesinger, A., & Furlanetto, S. R. 2008a, *MNRAS*, 385, 1348
- Mesinger, A., & Furlanetto, S. R. 2008b, *MNRAS*, 386, 1990
- Mesinger, A., & Furlanetto, S. 2009, *MNRAS*, 400, 1461
- Mesinger, A. 2010, *MNRAS*, 407, 1328
- Mesinger, A., Furlanetto, S., & Cen, R. 2011, *MNRAS*, 411, 955
- Miralda-Escude, J. 1998, *ApJ*, 501, 15
- Neufeld, D. A. 1990, *ApJ*, 350, 216
- Nilsson, K. K., Orsi, A., Lacey, C. G., Baugh, C. M., & Thommes, E. 2007, *A&A*, 474, 385
- Ouchi, M., et al. 2010, *ApJ*, 723, 869
- Partridge, R. B., & Peebles, P. J. E. 1967, *ApJ*, 147, 868
- Pawlik, A. H., Milosavljević, M., & Bromm, V. 2011, *ApJ*, 731, 54
- Raiter, A., Schaerer, D., & Fosbury, R. A. E. 2010, *A&A*, 523, A64
- Rakic, O., Schaye, J., Steidel, C. C., & Rudie, G. C. 2010, arXiv:1011.1282
- Rybicki, G. B., & Lightman, A. P. 1979, *New York, Wiley-Interscience*, 1979. 393
- Santos, M. R. 2004, *MNRAS*, 349, 1137
- Schaerer, D. 2002, *A&A*, 382, 28
- Schaerer, D. 2003, *A&A*, 397, 527
- Schaerer, D., & Verhamme, A. 2008, *A&A*, 480, 369
- Shimasaku, K., et al. 2006, *PASJ*, 58, 313
- Stanway, E. R., McMahon, R. G., & Bunker, A. J. 2005, *MNRAS*, 359, 1184
- Stanway, E. R., et al. 2007, *MNRAS*, 376, 727
- Stark, D. P., Ellis, R. S., Chiu, K., Ouchi, M., & Bunker, A. 2010a, *MNRAS*, 408, 1628
- Stark, D. P., Ellis, R. S., & Ouchi, M. 2011, *ApJ*, 728, L2
- Steidel, C. C., Erb, D. K., Shapley, A. E., Pettini, M., Reddy, N., Bogosavljević, M., Rudie, G. C., & Rakic, O. 2010, *ApJ*, 717, 289
- Trac, H., & Cen, R. 2007, *ApJ*, 671, 1
- Vanzella, E., et al. 2010, *A&A*, 513, A20
- Verhamme, A., Schaerer, D., & Maselli, A. 2006, *A&A*, 460, 397
- Verhamme, A., Schaerer, D., Atek, H., & Tapken, C. 2008, *A&A*, 491, 89
- Yan, H.-J., Windhorst, R. A., Hathi, N. P., Cohen, S. H., Ryan, R. E., O’Connell, R. W., & McCarthy, P. J. 2010, *Research in Astronomy and Astrophysics*, 10, 867
- Zahn, O., Mesinger, A., McQuinn, M., Trac, H., Cen, R., & Hernquist, L. E. 2010, arXiv:1003.3455
- Zel’Dovich, Y. B. 1970, *A&A*, 5, 84
- Zheng, Z., Cen, R., Trac, H., & Miralda-Escudé, J. 2010a, *ApJ*, 716, 574
- Zheng, Z., Cen, R., Trac, H., & Miralda-Escudé, J. 2010b, submitted to *ApJ*, arXiv:1010.3017